Environment International 176 (2023) 107989

Contents lists available at ScienceDirect

Environment International

journal homepage: www.elsevier.com/locate/envint

Full length article

Chitin and crawfish shell biochar composite decreased heavy metal bioavailability and shifted rhizosphere bacterial community in an arsenic/lead co-contaminated soil

Hanbo Chen [a,b,c,1], Yurong Gao [a,b,1], Huiyun Dong [d], Binoy Sarkar [e], Hocheol Song [f], Jianhong Li [g], Nanthi Bolan [h,i], Bert F. Quin [j], Xing Yang [k], Fangbai Li [l], Fengchang Wu [m], Jun Meng [b], Hailong Wang [a,n,*], Wenfu Chen [b,*]

[a] School of Environmental and Chemical Engineering, Foshan University, Foshan 528000, China
[b] Agronomy College, Shenyang Agricultural University, Shenyang 110866, China
[c] Institute of Eco-environmental Research, School of Environmental and Natural Resources, Zhejiang University of Science & Technology, Hangzhou 310023, China
[d] Institute of Soil and Water Resources and Environmental Science, College of Environmental and Resource Sciences, Zhejiang University, Hangzhou 310058, China
[e] Future Industries Institute, University of South Australia, Mawson Lakes, SA 5095, Australia
[f] Department of Earth Resources and Environmental Engineering, College of Engineering, Hanyang University, Seoul 04763, Korea
[g] Rubber Research Institute, Chinese Academy of Tropical Agricultural Sciences, Haikou 571101, China
[h] School of Agriculture and Environment, The University of Western Australia, Perth, WA 6001, Australia
[i] The UWA Institute of Agriculture, The University of Western Australia, Perth, WA 6001, Australia
[j] Quin Environmentals (NZ) Ltd., PO Box 125122, St. Heliers, Auckland 1740, New Zealand
[k] Key Laboratory of Agro-Forestry Environmental Processes and Ecological Regulation of Hainan Province, College of Ecology and Environment, Hainan University, Haikou 570228, China
[l] Institute of Eco-environmental and Soil Sciences, Guangdong Academy of Sciences, Guangzhou 510650, China
[m] State Key Laboratory of Environmental Criteria and Risk Assessment, Chinese Research Academy of Environmental Sciences, Beijing 100012, China
[n] Key Laboratory of Soil Contamination Bioremediation of Zhejiang Province, Zhejiang A&F University, Hangzhou 311300, China

A R T I C L E I N F O

Handling Editor: Dr. Hefa Cheng

Keywords:
Engineered biochar
Microbial community
Enzyme activity
Soil remediation
Structural equation model

A B S T R A C T

Sustainable management of ever-increasing organic biowaste and arable soil contamination by potentially toxic elements are of concern from both environmental and agricultural perspectives. To tackle the waste issue of crawfish shells and simultaneously minimize the threat of arsenic (As) and lead (Pb) to human health, a pot trial was conducted using chitin (CT), crawfish shell biochar (CSB), crawfish shell powder (CSP), and CT–CSB composite to compare their remediation efficiencies in As/Pb co-contaminated soil. Results demonstrated that addition of all amendments decreased Pb bioavailability, with the greatest effect observed for the CT–CSB treatment. Application of CSP and CSB increased the soil available As concentration, while significant decreases were observed in the CT and CT–CSB treatments. Meanwhile, CT addition was the most effective in enhancing the soil enzyme activities including acid phosphatase, α-glucosidase, N-acetyl-β-glucosaminidase, and cellobiohydrolase, whereas CSB-containing treatments suppressed the activities of most enzymes. The amendments altered the bacterial abundance and composition in soil. For instance, compared to the control, all treatments increased Chitinophagaceae abundance by 2.6–4.7%. The relative abundance of Comamonadaceae decreased by 1.6% in the CSB treatment, while 2.1% increase of Comamonadaceae was noted in the CT–CSB treatment. Redundancy and correlation analyses (at the family level) indicated that the changes in bacterial community structure were linked to bulk density, water content, and As/Pb availability of soils. Partial least squares path modeling further indicated that soil chemical property (i.e., pH, dissolved organic carbon, and cation exchange capacity) was the strongest predictor of As/Pb availability in soils following amendment application. Overall, CT–CSB could be a potentially effective amendment for simultaneously immobilizing As and Pb and restoring soil ecological functions in contaminated arable soils.

* Corresponding author at: School of Environmental and Chemical Engineering, Foshan University, Foshan, Guangdong 528000, China (H. Wang).
E-mail addresses: hailong.wang@fosu.edu.cn (H. Wang), wfchen5512@163.com (W. Chen).
[1] These authors contributed equally to this work and should be considered co-first authors.

https://doi.org/10.1016/j.envint.2023.107989
Received 16 January 2023; Received in revised form 8 May 2023; Accepted 21 May 2023
Available online 24 May 2023
0160-4120/© 2023 The Authors. Published by Elsevier Ltd. This is an open access article under the CC BY license (http://creativecommons.org/licenses/by/4.0/).

1. Introduction

The world is witnessing global contamination of agricultural soils caused by potentially toxic elements (PTEs). Highly accumulative PTEs in soils can disrupt soil structure, reduce soil fertility, render negative effects on plant growth and development (Chen et al., 2022b), and inhibit microbial activity (Xu et al., 2019), causing severe damage to ecological functions of the soil-biota system. This hinders efficient soil utilization, and further poses potential threats to food security and human health (Hou et al., 2020). The introduction of PTEs into the human body through inhalation, ingestion, and dermal contact poses a significant threat to human health by disrupting organ function and endocrine systems (Mehmood et al., 2019; Mehmood et al., 2021). Arsenic (As), cadmium (Cd), and lead (Pb) have been identified as major etiological factors for causing cancer, myocardial infarction, and pulmonary diseases, etc. in humans (Ahmad et al., 2019). Considering the bio-toxicity, frequency of occurrence, and potential risk of human exposure to PTEs found at National Priorities List sites, the Agency for Toxic Substances and Disease Registry (ATSDR) of the United States prioritized As (1,676 points) and Pb (1,531 points) as the top two elements in the Substance Priority List (ATSDR, 2019). In China, a nationwide survey showed that 19.4% of the sampled arable soil was contaminated with various PTEs exceeding China's soil environmental quality limits, among which As and Pb ranked third (2.7%) and sixth (1.5%) (Zhao et al., 2015). Hence, the reclamation of As/Pb contaminated soil is a need of the hour to safeguard the sustainable development of exhausted soil resources and protect eco-environmental health. The *in-situ* immobilization technique using (in)organic amendments (e.g., manure, compost, lime, fly ash, metal oxides, and biochar) has been proposed as a gentle remediation strategy for the management of contaminated sites to mitigate the potential human health risk of PTEs, with the advantages of being environmentally benign and cost-effective (Hou et al., 2020; Liu et al., 2022). Nevertheless, the utilization of a single soil amendment in the remediation of As/Pb co-contaminated soils is highly controversial because these amendments may immobilize Pb while increasing As mobility (Pan et al., 2021; Wen et al., 2021; Yang et al., 2022a). Therefore, it is of significance to screen a multifunctional amendment that can concurrently immobilize Pb and As in co-contaminated soils and achieve ecological restoration of PTEs-spoiled areas.

On the other hand, rapid economic development worldwide has led to the ever-increasing consumption of aquatic crustaceans (Chen et al., 2020b). Globally, 6–8 million tonnes of waste shells from crabs, lobsters, and crawfish are annually generated (Yan and Chen, 2015), particularly from Asian countries (Bai et al., 2022). Among them, crawfish (*Procambarus clarkii*) is one of the common aquatic products receiving great popularity in China. However, the quick accumulation of shell waste along with the large-scale consumption of crawfish in China has led to critical environmental issues and recycling pressure (Chen et al., 2022e), requiring safe and sustainable waste management practices to reduce negative environmental impacts. Such practices include converting shell waste into functional materials such as mechanically-ground crawfish shell powder (Yang et al., 2022a), chemically-extracted chitin (Ahmed et al., 2020), and thermally-produced biochar (Sun et al., 2021; Zhang et al., 2022). Chitin is a polysaccharide substance that can be extracted from crustacean shells, with a unique cationic character originated from the hydrolysis of surface acetyl groups (Fig. S1), which imparts good binding properties toward metal(loid)s via chelation/complexation (Bai et al., 2022), particularly for anionic metalloids such as As (Yang et al., 2015). Biochar refers to a carbon-rich product from the pyrolysis of biomass with limited or no oxygen supply (Lehmann et al. 2011; Gao et al., 2023). Crawfish shell biochar has been used as an effective remediation material in the adsorption/immobilization of metal cations including Pb via cation exchange and mineral precipitation mechanisms (Sun et al. 2021). Nevertheless, the pristine crawfish shell biochar owns a negatively charged surface that impedes interfacial interaction with negatively charged As species. Furthermore, both chitin and biochar have been considered as fertilizers and effective soil conditioning agents in agricultural and environmental applications (Shamshina et al., 2020; Gao et al., 2022; Yang et al., 2022a). Therefore, the combination of chitin and biochar might be an efficient strategy to synergize the advantageous characteristics of both resource materials in environmental decontamination and soil quality improvement. However, no information is available on the reclamation of co-contaminated soils by simultaneously immobilizing cationic Pb and anionic As and improving soil properties using a chitin–biochar composite to date. To our knowledge, this investigation is the first attempt to test the feasibility of using such composites to remediate PTEs-spoiled soil, particularly for As/Pb co-contaminated soil.

In addition, soil microorganisms are crucial indicators reflecting the status of soil fertility, health, and environmental stresses present in a system (Xu et al., 2019). The activity of soil microorganisms in the rhizosphere is of great importance for promoting crop growth, especially in heavy metal-contaminated soils (Bandara et al., 2022). Excessive concentration of heavy metals accumulated in the soil could induce bio-toxicity towards microbiota and inhibit their abundance, diversity and activities (Pan et al., 2021). Soil microorganisms in turn could change their community structure in response to the new habitation under continuous stress (Zhu et al., 2022). Soil amendments can alter soil chemical, physical and biological properties which directly affect the development of microorganisms and metal(loid) behaviors such as (im) mobilization, dissolution, and redox transformation. Understanding the amendment-induced change of rhizosphere bacterial community is the key to reveal the remediation mechanisms in an amendment-metal (loid)-microorganism system. However, the interactive effects of chitin–biochar composites on soil microbial abundance and community composition, particularly in metal(loid)-contaminated rhizosphere soil, are still largely unknown.

It was hypothesized that the chitin-crawfish shell biochar composite might simultaneously immobilize As and Pb via chitin-As chelation and biochar-Pb precipitation/complexation, improve the soil quality, alter bacterial community structure, and promote plant growth. In view of this hypothesis from the perspectives of biowaste utilization and environmental pollution control, a pot experiment using radish (*Raphanus sativus* L.) as a model plant was designed to examine the effect of different crawfish shell-derived immobilizing agents for the remediation of As/Pb co-contaminated soil. Hence, to provide scientific insights into this innovative strategy, the overall aim of this study is to fill the knowledge gap about chitin-biochar composite mediated-phytoavailability of As and Pb in the soil–plant system. The specific objectives are to: (1) determine and compare the efficiency of four amendments derived from crawfish shells, i.e., crawfish shell powder, chitin, crawfish shell biochar, and chitin-biochar composite application on the bioavailability, fractionation, and accumulation of As/Pb in the soil-plant system, (2) investigate the influence of such amendments on soil properties, soil fertility, enzyme activity, and plant growth, (3) evaluate the changes in soil bacterial abundance and community composition in response to different amendments, and (4) establish a correlation between the measured parameters to predict the key environmental factor(s) affecting the availability of As and Pb.

2. Materials and methods

2.1. Soil sampling

A paddy soil co-contaminated by As and Pb was sampled from the 0–20 cm surface layer in Shaoxing City, China (30°00′N, 120°79′E). As reported in our previous study (Pan et al., 2021), the total concentration was 736 mg kg^{-1} for Pb and 141 mg kg^{-1} for As, which exceeded the risk screening level (100 and 30 mg kg^{-1} for Pb and As, respectively) regulated by the Soil Environmental Quality Standard GB15618-2018 in China. The collected soil was air-dried, ground (3 mm), and stored under dry conditions before the pot experiment. Detailed basic properties of the selected soil (Table S1) and characterization methods can be found in the Supplementary Material.

2.2. Amendments preparation and characterization

The crawfish shells were collected from an aquatic product market located in Hangzhou City, China. These shells were thoroughly rinsed using tap water, and then oven-dried at 80 °C for 24 h. A part of dried shells was ground and sieved (60 mesh) to obtain the crawfish shell powder (CSP). The other portion of the shells was pyrolyzed in a pyrolysis furnace at 650 °C for 2 h to produce crawfish shell biochar (CSB). Once the furnace was cooled down, the CSB was retrieved, ground (60 mesh), and stored under dry conditions before further analysis and experiments. Practical-grade crawfish-derived chitin ($(C_8H_{13}NO_5)_n$; CT) was purchased from Hangzhou Junying Co., LTD and used without any further purification. To prepare the CT–CSB composite, CT and CSB (1:1, w/w) were ground and mixed well in an agitator at 200 rpm for 2 h.

The key physicochemical properties of selected amendments, i.e., pH, ash content, and cation exchange capacity, were measured according to a previous study (Chen et al., 2022c). In addition, microscopic, spectroscopic, and crystal structure characterization of selected amendments were carried out by using scanning electron microscope/energy-dispersive X-ray spectrometry (SEM/EDS), Fourier transform infrared (FTIR) spectrometry, and X-ray diffraction (XRD) analyses, respectively. Detailed information for the characterization procedures can be found in the Supplementary Material. Results of selected properties and spectroscopic analyses of these amendments have been reported (Yang et al., 2022a) and presented in Table S4 and Fig. S2.

2.3. Pot experiment setting

A radish (*Raphanus sativus* L.) growth experiment was conducted in a greenhouse at Zhejiang A&F University, China. The pot experiment was conducted under the following controlled conditions: temperature (27 ± 3 °C), humidity (65 ± 5%), and light (8/16 h light/dark cycle). Each pot (diameter: 23 cm, height: 14 cm) was filled with 3 kg of the As/Pb-contaminated soil. Then 1% CSP, CT, CSB, and CT–CSB were applied individually to each pot. The soil and amendment in the pot were homogenously mixed and supplemented with KH_2PO_4 and urea at a dose of $K_2O = 0.2$ g·kg^{-1}, $P_2O_5 = 0.32$ g·kg^{-1}, and N = 0.25 g kg^{-1} (Chen et al., 2020a). The contaminated soil without any amendment was set as the control. In total, the pot experiment consisted of five treatments (i.e., control, CSP, CT, CSB, and CT–CSB) and each treatment replicated three times. Randomized block design was adopted to arrange the total 15 pots. At the first three days, all pots were watered using deionized water to keep soil moisture nearly saturated. Afterwards, ten seeds of radish were sown into each pot, and five healthy seedlings were kept after thinning. After 50-day maturity, radish was harvested and divided into two parts (i.e., shoot and root). The plant samples were first rinsed with tap water to get rid of the attached soil particles thoroughly, then these samples were rinsed three times using deionized water, and oven-dried at 105 °C for 30 min, followed by further oven-drying at 65 °C for 24 h. Dried plant samples were ground (100 mesh) and stored prior to further analysis. The fresh rhizosphere soil from each pot was sampled, a portion of sub-sample was used to analyze microbial biomass carbon/nitrogen and enzyme activities of soil, and the other part of fresh soil was immediately stored in an ultra-low temperature freezer at −80 °C for the analysis of bacterial community of the soil. The soil left in the pot was also collected, air-dried, and ground (10 and 100 mesh) for subsequent analyses.

2.4. Soil analysis

2.4.1. Soil property, nutrient availability, and enzyme activity

In this study, the soil samples retrieved after harvesting were subject to physical (bulk density, water content), chemical (pH, cation exchange capacity (CEC), and dissolved organic carbon (DOC)), and biological (microbial biomass carbon/nitrogen (MBC/MBN)) properties. In addition, the concentrations of available N and P were measured to assess soil fertility. The physicochemical properties and nutrient availabilities of soil were assessed as per Lu (2000). The MBC and MBN of soil were measured using the chloroform fumigation extraction method as reported by Wu et al. (1990).

The activities of five typical soil enzymes including C-acquiring enzymes (α-glucosidase, AG, EC 3.2.1.20; β-xylosidase, XYL, EC 3.2.1.37; cellobiohydrolase, CB, EC 3.2.1.91), N-acquiring enzyme (N-acetyl-β-glucosaminidase, NAG, EC 3.2.1.30), and P-acquiring enzyme (acid phosphatase, AP, EC 3.1.3.1) were analyzed. The activities of these enzymes were measured by analyzing the yields of the fluorescent cleavage products, i.e., 4-methylumbelliferyl (MUB) or 4-methylcoumarin (MUC) as described by Saiya-Cork et al. (2002). Geometric mean enzyme activity (GMEA) is a general index that allows integration of information from variables with different units and ranges of variation (Chen et al., 2019). GMEA was calculated as $GMEA = (AG \times XYL \times CB \times NAG \times AP)^{1/5}$. More details about soil characterization methods are provided in the Supplementary Material.

2.4.2. Metal(loid)s availability and redistribution

The total Pb/As content of the soil was determined by digesting the soil with $HF–HClO_4–HNO_3$ (Carignan and Tessier, 1988), and quantified using inductively coupled plasma optical emission spectroscopy (ICP-OES Optima 2000, PerkinElmer Co., USA). Diethylenetriaminepenta-acetic acid (DTPA) and $NH_4H_2PO_4$ were selected as the extractants for the determination of potentially available Pb and As in the soil, respectively. Furthermore, Tessier (Tessier et al., 1979) and Wenzel sequential extraction procedure (Wenzel et al., 2001) were employed for analyzing the fractions of Pb and As in the soil, respectively. Detailed information on the extraction of available Pb/As and their fractional quantification are included in the Supplementary Material (Section S1.4).

2.4.3. DNA extraction and qPCR amplification

DNA extraction and qPCR analysis of frozen soil samples were completed by Shanghai Majorbio Bio-Pharm Technology Co., Ltd. Total DNA was extracted from 0.35 g of soil sample using E.Z.N.A.® soil DNA Kit (Omega Bio-tek, Norcross, GA, U.S.) following the instructions of the manufacturer's protocol (An et al., 2022; Xie et al., 2022). The extracted DNA concentration and purity were determined using a NanoDrop 2000 spectrophotometer (Thermo Fisher Scientific, Waltham, MA, USA). DNA integrity was examined on 1% agarose gels and stored at −20 °C for further analyses. The detailed information including primers, annealing temperature, and amplification information of all target genes are described in the Supplementary Materials.

2.4.4. High-throughput sequencing analysis

Microbial diversity analysis was conducted using Illumina high-throughput sequencing (Shanghai Majorbio Bio-Pharm Technology Co., Ltd). The V3-V4 region of the bacterial 16S rRNA gene was amplified with special primers (338F and 806R). The pre-treated sequences were grouped into operational taxonomic units (OTUs), after which clustering analysis of the optimized sequence adopting 97% identity thresholds was performed using the USEARCH software (Version 11.0). Obtained data were analyzed and graphed on the Majorbio Cloud Platform (https://www.majorbio.com). Alpha diversity indices include OTU number, Simpson, and Ace. Venn and nonmetric multidimensional scaling (NMDS) analyses were performed based on the Bray-Curtis distance metric. Redundancy analysis (RDA) was performed to determine environmental factors influencing soil bacterial community composition. Welch's *t*-test in STAMP was used to identify the significant difference in relative abundances at the family level between treatments.

2.5. Plant analysis

The dry biomass of plant was recorded. The N concentration in plants was measured using an elemental analyzer (Flash EA1112, Thermo Finnigan, Italy). Nitric acid (HNO_3) was employed to digest the plant shoots and roots, and the P content in the digestates was measured by molybdenum blue method on a spectrophotometer at 700 nm (Lu, 2000), and the As/Pb concentration in the plant digestates were quantified by ICP-OES.

2.6. Data quality and statistical analysis

All reagents used in the experiments were of analytical grade. The plasticware and glassware used in the experiment were soaked in 5% nitric acid overnight prior to use. Ultra-pure water (18.2 MΩ cm^{-1}, ULPHW-I, Ulupure Co. LTD., China) was used for all analyses, and all devices were calibrated and uncertainties were calculated to ensure the accuracy of experimental data. The quality control for the determination of available nutrients and As/Pb concentrations in the soil and plant samples were conducted by comparing them to the certified reference materials (GBW-07405 for soil and GBW-07603 for plant). The recovery percentage of As and Pb in sequential extraction was 89.5–95.8% and 80.2–85.7%, respectively. The ICP-OES was recalibrated after the measurement of each 30 samples, and the detection limit for As/Pb was 0.01 mg L^{-1} (i.e., 0.01 ppm).

The raw data were statistically analyzed using IBM SPSS Statistics 26 software. The distributional characteristics of obtained data were assessed for normality using the Shapiro-Wilk test. Analyses of variance (ANOVA) and Duncan's multiple range test were employed to assess significant differences between treatments ($P < 0.05$). Pearson's correlation analysis between variables was performed with a significance level of $P < 0.05$ and $P < 0.01$. Partial least squares path modeling (PLS-PM) was performed using the "plspm" package in R studio to further estimate relationships and contributions among environmental variables and As/Pb availability. The estimates of the coefficient of determination (R^2) and path coefficients (β) were validated by using 5000 bootstrap numbers. The "Goodness-of-Fit" (GoF) statistics were used as the predictive parameter to assess the path model.

3. Results

3.1. Soil properties

As shown in Table 1, compared to the control, application of four amendments decreased the soil bulk density by 5.3–10.6%, while significant increases in soil water content in all treatments were observed, ranging from 10.2% to 30.4%. Regarding soil chemical properties, except for the CT treatment, all treatments increased soil pH and CEC. Specifically, the soil pH increased by 1.0–1.4 units after the incorporation of amendments (except CT). The CSP, CSB, and CT–CSB treatments resulted in enhanced CEC of soil with a non-significant ($P > 0.05$) difference among them. In addition, except for CSP, the amendments increased the DOC content in the soil, and the maximum enhancement corresponded to the CSB-treated soil (up to 33.2%). Furthermore, the amendments also increased the contents of MBC and MBN by 1.7–11.1 folds and 1.0–2.5 folds, respectively, as compared to the control (Table 1).

3.2. Nutrient phytoavailability and plant yield

Fig. 1A shows significant improvements in soil-available N concentration in the CSP (by 45.5%) and CT (by 89.5%) treatments, compared to the control. Interestingly, the concentrations of N in the plant root in these treatments significantly decreased compared to that of the control (Fig. 1B). However, the N contents in the shoot of radish were found to be significantly higher in the CT and CT–CSB treatments, which respectively increased by 54.5% and 43.4% than the control (Fig. 1B). Regarding available P concentration in soil, CSP was more effective with an increase of up to 1.1-fold, which was much higher than that of CSB (24.1%) and CT–CSB (30.0%) (Fig. 1C). As expected, the highest P accumulation in plant root corresponded to the CSP treatment, with the values increased by 1.61-fold (Fig. 1D). The P concentration in plant shoot increased after the application of CSP, CT, and CT–CSB; however, a non-significant difference ($P > 0.05$) was observed among these treatments.

All amendments increased the dry weight of radish root, and the highest promotion of plant yield was associated with CT–CSB treatment, increased by 65.9% compared to the control (Fig. 2). The plant shoot biomass exhibited a trend similar to that of the root; the effectiveness of amendments followed a descending order of CT–CSB (74.9%) > CSB ≈ CSP ≈ CT (54.1–54.6%), as compared to the control (Fig. 2).

3.3. Bioavailability, accumulation, and fractionation of Pb

Application of all amendments led to significant decreases in available Pb in the soil, by 18.8% for CSP, 9.9% for CT, 47.6% for CSB, and 46.5% for CT–CSB, as compared to the control (Fig. 3A). Accordingly, the Pb uptake in plant was decreased by 46.2–62.1% in shoot and 30.7–53.0% in root of radish (Fig. 3B). CSB-containing amendments (i.e., CSB and CT–CSB) were found to be the most effective treatments in decreasing the bioavailability of Pb in the soil, wherein there was no significant difference between CSB- and CT–CSB-mediated responses to immobilization and plant accumulation of Pb (Fig. 3A, B).

The geochemical fractions and associated concentrations of Pb are shown in Fig. 3C and Table S5. The proportions of mobile fractions, i.e., sum of Pb_{ex} and Pb_{ca}, were found to be lower after all amendment applications, and the maximum reduction (12.6%) was observed in the CSB treatment, compared to the control (Fig. 3C). As for Pb_{or}, only CSB

Table 1
Influence of different amendments on soil properties.

Treatment	Bulk density (g cm^{-3})	Soil water content (%)	pH	Cation exchange capacity (cmol kg^{-1})	Dissolved organic carbon (g kg^{-1})	Microbial biomass carbon (mg kg^{-1})	Microbial biomass nitrogen (mg kg^{-1})
Control	1.39 ± 0.04 a	20.91 ± 1.05 d	6.48 ± 0.03 c	11.55 ± 0.10 b	0.43 ± 0.05 b	64 ± 5 e	10.42 ± 2.62 c
CSP	1.32 ± 0.02 b	23.06 ± 0.58 c	7.89 ± 0.01 a	11.79 ± 0.07 a	0.46 ± 0.03 b	335 ± 62 c	28.28 ± 8.20 ab
CT	1.31 ± 0.02 b	27.27 ± 1.31 a	6.65 ± 0.17 c	11.44 ± 0.03 b	0.54 ± 0.03 a	173 ± 16 d	22.38 ± 5.36 b
CSB	1.24 ± 0.03 c	23.13 ± 0.62 c	7.73 ± 0.10 a	11.86 ± 0.14 a	0.57 ± 0.02 a	531 ± 72 b	36.67 ± 4.72 a
CT–CSB	1.26 ± 0.01 c	25.09 ± 0.58 b	7.52 ± 0.11 b	11.93 ± 0.07 a	0.55 ± 0.03 a	776 ± 82 a	21.33 ± 1.68 b

Control: untreated contaminated soil; CSP: crawfish shell powder; CT: chitin; CSB: crawfish shell biochar; CT–CSB: chitin-crawfish shell biochar composite. The results were given as mean ± standard deviation. Different letters indicate significant ($P < 0.05$) difference between treatments.

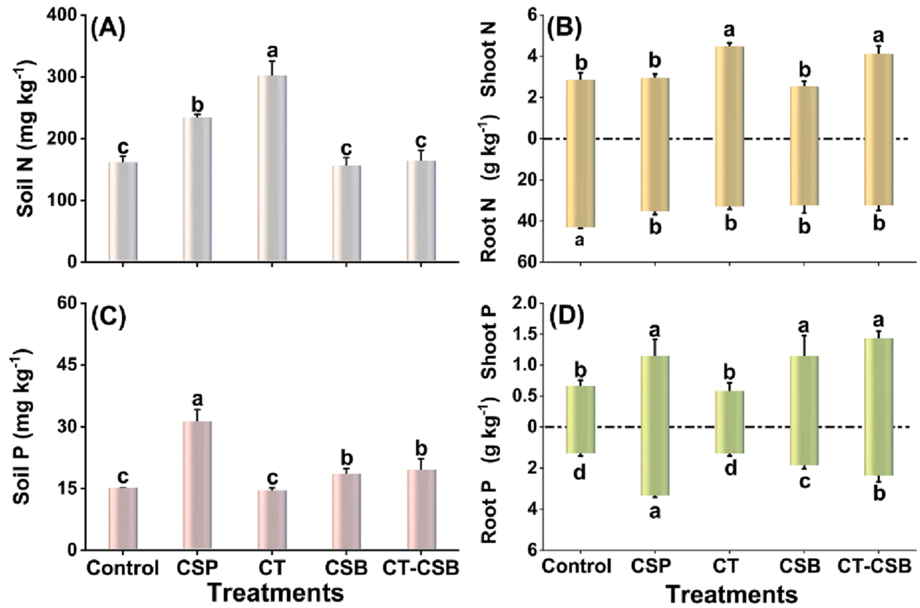

Fig. 1. Available N in the soil (A) and N uptake in plants (B); Available P in the soil (C) and P uptake in plants (D). Control: untreated contaminated soil; CSP: crawfish shell powder; CT: chitin; CSB: crawfish shell biochar; CT–CSB: chitin-crawfish shell biochar composite. Error bars indicate standard deviation of the means (n = 3), with different letters indicating significant ($P < 0.05$) difference between treatments.

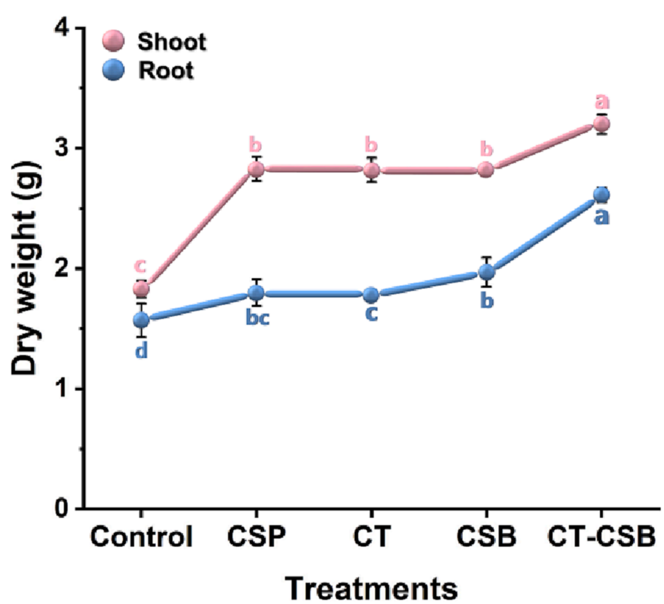

Fig. 2. Plant biomass under different amendments (D). Control: untreated contaminated soil; CSP: crawfish shell powder; CT: chitin; CSB: crawfish shell biochar; CT–CSB: chitin-crawfish shell biochar composite. Error bars indicate standard deviation of the means (n = 3), with different letters indicating significant ($P < 0.05$) difference between treatments.

application significantly increased by 32.7% higher than that of the control (Table S5). Additionally, except for CT treatment, the concentrations of Pb_{re} fraction in the other treatments increased by 19.8–28.9% (Table S5), and the proportion of Pb_{re} increased by 7.1–10.6% (Fig. 3C), as compared to the control. Overall, the application of amendments aided the transformation of mobile Pb fractions into stable Pb fractions to varying degrees.

3.4. Bioavailability, accumulation, and fractionation of As

Various amendments caused contradictory effects on the potentially bioavailable As concentration in soils (Fig. 4A). Compared to the control, the available concentrations of As in the soil treated with CT and CT–CSB decreased by 31.4% and 29.8%, respectively, whereas the applications of CSP (25.7%) and CSB (32.6%) significantly increased the availability of As. For the As uptake by plant root, significant reductions were noted in all treatments, resulting in decreases by 20.0–46.4%, compared to the control (Fig. 4B). Furthermore, the trend of As accumulation in the plant shoot was similar to that in the root. For instance, all amendments except for CSP decreased the As uptake in plant shoots, and the maximum reduction was noted in the CT treatment, with a decrease of 51.4% (Fig. 4B).

Regarding the five extracted fractions of As in soils after amendments, the associated results are presented in Fig. 4C and Table S6. Application of CT decreased the mobile fraction of As (sum of As_{nsa} and As_{sa}) by 2.1%, whereas significant increases were observed in the CSP (5.5%) and CSB (0.7%) treatments, as compared to the control (Fig. 4C). The CT–CSB treatment caused a reduction (35.1%) of the As_{nsa} concentration but had little influence on the As_{sa} fraction, as compared to the control (Table S6). Moreover, application of CT and CT–CSB significantly increased the concentration of As_{cr} (24.2% and 16.7%, respectively) and As_{re} (7.5% and 3.8%, respectively) (Table S6). In addition, a significant reduction in As_{cr} proportion was noted from 35.8% to 26.9% in the CSP treatment (Fig. 4C).

3.5. Soil enzyme activities

The application of four treatments had similar effects on the activities of AG, XYL, and CB. As compared to control, CT addition caused significant improvements for AG (12.6%) and CB (39.3%); however, CSB-containing treatments suppressed the activities of AG, XYL, and CB, with decreases of 14.6–25.6%, 23.7–27.4%, and 28.7–38.1%, respectively (Fig. 5A, 5B, 5C) compared to the control. For the NAG, all amendments significantly enhanced its activity, following the order of the control < CSP < CT–CSB < CSB < CT, with an increase ranging between 4.4 and 15.5 folds compared to the control (Fig. 5D). In the case of AP, a 25.5% increase of AP activity was found in the CT treatment, whereas the CSP and CSB applications suppressed the activity of AP by approximately 27%, relative to the control (Fig. 5E). The increased GMEA of soil were found in all amendments, and the maximum

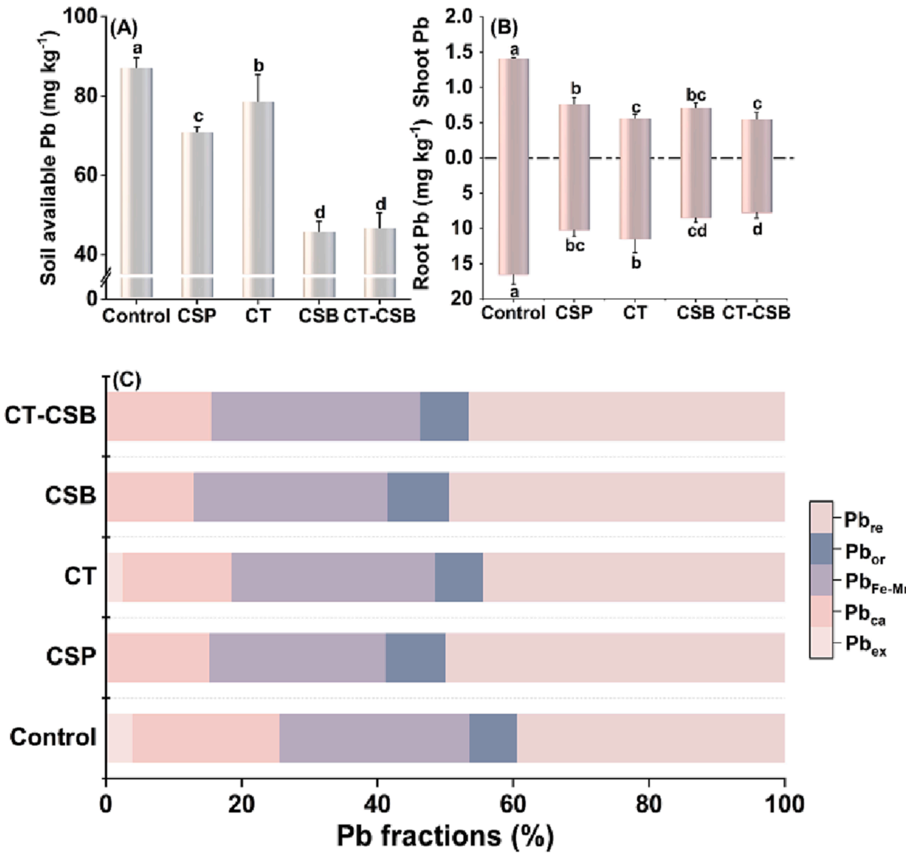

Fig. 3. Soil available Pb (A), uptake of Pb in plant shoots and roots (B), and soil Pb fractions (C). Control: untreated contaminated soil; CSP: crawfish shell powder; CT: chitin; CSB: crawfish shell biochar; CT–CSB: chitin-crawfish shell biochar composite. Error bars indicate standard deviation of the means (n = 3), with different letters indicating significant ($P < 0.05$) difference between treatments.

enhancement (103%) corresponded to the CT treatment, whereas there was no significant difference in the increment in CSP, CSB, and CT–CSB treatments (Fig. 5F).

3.6. Soil bacterial communities

The similarity in OTU overlap (1011 OTUs) among all treatments (including control) was analyzed by Venn diagrams (Fig. S3A). The number of unique OTU was found to decrease in all treatments compared to the control. The composition of soil bacterial communities varied significantly among the amendments (stress = 0.023, $P = 0.001$) (Fig. S3B). As shown in Table S7, there was no significant difference in the diversity of soil bacterial communities among four amendments with Simpson index, while Ace diversity metrics were much higher ($P < 0.05$) in the CT treatment compared to other groups. Additionally, applications of CT and CT–CSB significantly increased the bacterial 16S rRNA gene copy numbers, by 1.96 and 1.25 folds, respectively, compared to the control (Table S7).

At phylum level, the composition of soil bacterial communities was dominated by Proteobacteria, followed by Bacteroidota, Firmicites, and Acidobacteriota among treatments (Fig. S4), and the relationship between different amendments and bacterial species was presented using circos diagram (Fig. S5). For instance, except for the CSP, application of other amendments increased the relative abundance of Proteobacteria (14.7–19.7%), whereas it resulted in decrease of the relative abundances of Acidobacteriota (8.4–11.4%) and Chloroflexi (2.3–2.7%), compared to the control. To further analyze the variation in community composition, predominant bacteria at family level were determined (Fig. 6A). A significant enhancement of Chitinophagaceae abundance (2.61–4.69%) was observed among all treatments, and the highest increase was associated with CT treatment. The relative abundance of Oxalobacteraceae increased by 5.26% and 6.66% in the CT and CSB treatments, respectively. In addition, CSB application also increased the proportions of Caulobacteraceae (2.42%) and Microscillaceae (3.20%) as compared to the control. Furthermore, the relative abundance of Comamonadaceae in the CT–CSB treatment increased by 2.11%, while that of CSB treatment was found to be 1.60% lower than the control (Fig. 6A). Redundancy analysis (RDA) was conducted to identify the crucial soil variables influencing bacterial community composition (Fig. 6B). Soil bulk density, water content, available As, and available Pb had significant ($P < 0.05$) effects on the composition of soil bacterial communities. Pearson's correlation analysis was also employed to reveal the correlation between the main categories of bacteria and environmental factors (Fig. 6C). For instance, soil bulk density was negatively correlated to the relative abundance of Caulobacteraceae, Oxalobacteraceae, and Chitinophagaceae, whereas soil water content had a positive correlation with Chitinophagaceae, and Comamonadaceae. The soil available As or Pb was negatively correlated with Oxalobacteraceae abundance, while available Pb also showed a negative correlation with the abundance of Caulobacteraceae.

3.7. Linkages among soil properties, soil fertility, bacterial community, and metal(loid)s availability

Pathway analysis using PLS-PM model provided good fits to the environmental variables with a Goodness-of-Fit index of 0.622, which explained 58% and 90% of the variances in the soil available As and Pb concentrations, respectively (Fig. 7). Specifically, the amendments had a direct positive effect on soil chemical (i.e., pH, DOC, and CEC) and biological (MBC and MBN) properties with path coefficient (β) of 0.535

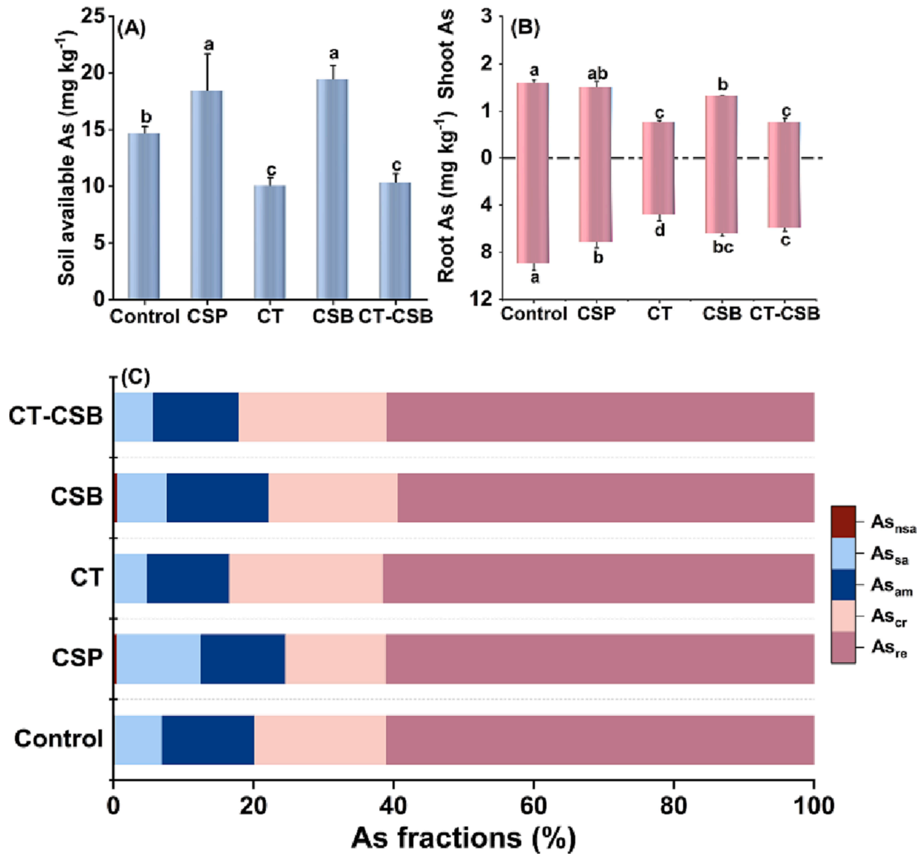

Fig. 4. Soil available As (A), uptake of As in plant shoots and roots (B), and soil As fractions (C). Control: untreated contaminated soil; CSP: crawfish shell powder; CT: chitin; CSB: crawfish shell biochar; CT–CSB: chitin-crawfish shell biochar composite. Error bars indicate standard deviation of the means (n = 3), with different letters indicating significant ($P < 0.05$) difference between treatments.

and 0.861, respectively. This indicates that the impact of amendment application on biological properties was greater than on chemical properties. Of note, the soil chemical properties negatively (β = -0.411) affected Pb availability but positively (β = 0.837) affected As availability in the soil. As calculated by the standardized total effects (Fig. S6), soil chemical property was the strongest predictor influencing As/Pb availability, followed by the soil biological property.

4. Discussion

4.1. Response of soil properties to amendments

Amending porous materials such as biochar into soils contributes to the reduction of soil bulk density (Singh et al., 2022), hence the reduction in bulk density was mainly caused by the relatively high pore surface area (9.7–16.0 m^2 g^{-1}) and pore volume (0.02–0.05 cm^3 g^{-1}) of the applied amendments, thereby increasing the microporosity of the soil. Furthermore, the decrease in soil bulk density contributed to the increase in water retention capacity of the soil (Dai et al., 2020). Of note, the most effective improvement of soil water content corresponded to the CT treatment, which was due to the excellent moisture-retention ability of high-molecular-weight chitin (Sirajudheen et al., 2021). The enhancement of soil pH in the CSP, CSB, and CT–CSB treatments was attributed to the high pH of CSP (pH 8.7) and CSB (pH 10.6) (Table S4), along with the release of alkali salts from the amendments (Wen et al., 2021). The observed increase in soil CEC after amendments application could be attributed to intrinsic high CEC of the amendments associated with surface alkalinity and high ash content (Chen et al., 2020a; Dai et al., 2020), as demonstrated in Table S4.

The reason for the increased DOC in amended soils could be ascribed to the direct input of DOC, the entrapment of indigenous DOC by amendments, and the change in soil properties (e.g., pH) (Yang et al., 2022c). Moreover, labile C could be rapidly incorporated into the microbial biomass through the microbial metabolism (Cotrufo et al., 2015), as evinced by the enhancement of MBC (Table 1). MBC and MBN are biological indicators reflecting the relatively labile soil carbon/nitrogen pool which can be easily utilized by soil microorganisms (Zhao et al., 2021). Therefore, the increases of MBC and MBN could be attributed to favorable habitat improvement (e.g., soil moisture, aeration, and temperature) for soil microorganisms after amendments (Situ et al., 2022).

4.2. Nutrient availability and accumulation

The increased N availability in CSP and CT treatments was expected because chitin has been reported as a nitrogen-releasing fertilizer (Shamshina et al., 2020). Moreover, it could function as C and N resources for microbial growth and enhance the N-related enzyme activity (e.g., N-acetyl-β-glucosaminidase) (Fig. 5D), consequently promoting soil N cycles. The N content (1.3%) of CSB was low, with most of N is likely present as non-bioavailable form due to the loss of N at high temperature condition during pyrolysis (650 °C in this study) (Chen et al., 2020a). This limited availability of N likely had a negligible influence on soil N availability in the CSB treatment. Meanwhile, addition of CT increased the soil available N concentration, whereas the effect of CT–CSB addition was not apparent. The co-occurrence of biochar may have potentially immobilized inorganic N derived from chitin mineralization through surface chemisorption, as suggested by Gao et al. (2019). Furthermore, all treatments caused reductions in N uptake by plant roots, this might be attributed to the “dilution effect” resulted from

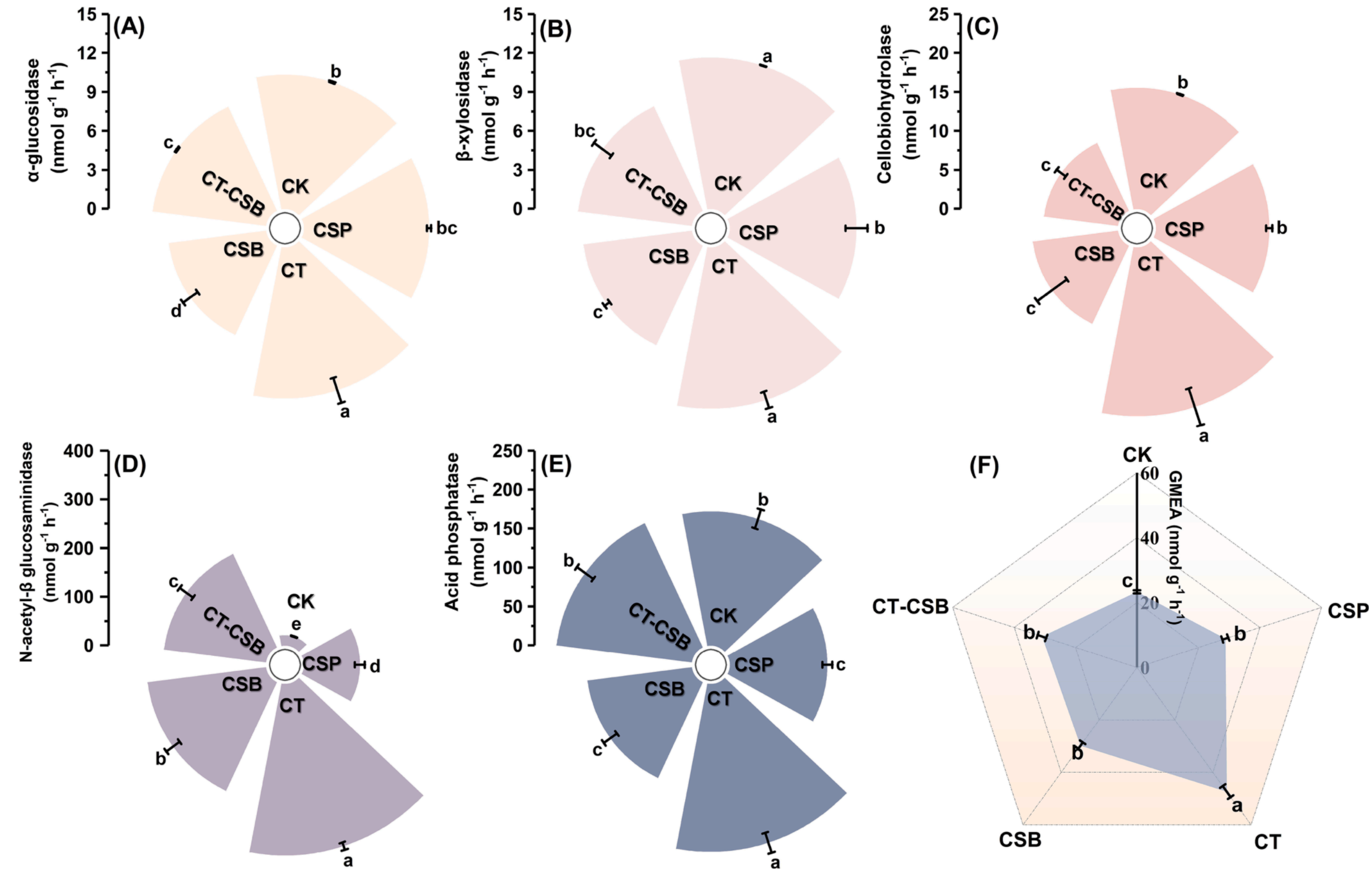

Fig. 5. Soil enzyme activities: α-glucosidase (A), β-xylosidase (B), cellobiohydrolase (C), N-acetyl-β-glucosaminidase (D), acid phosphatase (E), and geometric mean enzyme activity (GMEA) (F). CK: untreated contaminated soil; CSP: crawfish shell powder; CT: chitin; CSB: crawfish shell biochar; CT–CSB: chitin-crawfish shell biochar composite. Error bars indicate standard deviation of the means (n = 3), with different letters indicating significant ($P < 0.05$) difference between treatments.

the increased plant biomass (Fig. 2). In addition, we also assume that CT could facilitate nitrogen uptake efficiency, promoting the transfer of adsorbed N from root to shoot. In a study by Egusa et al. (2020), the authors found that chitin could alter the expression levels of genes linked to nutrient absorption, assimilation and photosynthesis in tomato, thereby increasing the efficiency of N uptake by plants.

The improvement of P availability in CSP and CSB treatments could be linked to the direct supply of exogenous P from the amendments because crawfish shells are rich in available P (Fig. S2B) (Yang et al., 2022c). Additionally, the elevated soil pH (Table 1) after amendment likely caused complexation of Fe/Al ions with OH^- ions in the soil, facilitating the release of surface-bound phosphate (Wang et al., 2022). It was also assumed that the amendment could improve the microbial habitat for microorganisms, which in turn enhances the conversion of organic P into plant-available P (Wang et al., 2022). However, according to the acid phosphatase activity and soil available P concentration in response to amendment application, this indirect pathway might have little influence.

4.3. *Amendment-induced (im)mobilization of metal(loid)s*

4.3.1. *Lead*

To varying degrees, all amendments facilitated the transformation of soil mobile Pb fractions to stable Pb fractions, thus reducing the bioavailability and bioaccumulation of Pb (Fig. 3). The stabilization of Pb by the amendments is assumed to involve following potential mechanisms. First, since Pb mobility and availability are closely related to the soil pH, the rise of soil pH caused by the amendments could aid in Pb immobilization (Pan et al., 2021), by inducing precipitation into $Pb(OH)_2$ and by enhancing electrostatic attraction to the negatively-charged binding sites at elevated pH condition (Chen et al., 2022b). Second, the ash content of amendment can greatly affect the adsorption behavior of Pb through cation exchange and metal-mineral precipitation (Sun et al., 2021). Both CSP and CSB have rich metal cations (e.g., Ca^{2+}, Mg^{2+}, and K^+) (Fig. S2B), which promoted cation exchange reaction with Pb^{2+} (Sun et al., 2021). The pathway analysis also supported that the soil chemical properties (i.e., pH, CEC, DOC) had a direct effect on reducing Pb availability (Fig. 7). Furthermore, carbonate in CSP/CSB (Fig. S2C) could react with Pb^{2+} to form $PbCO_3$, which contributed to Pb immobilization (Pan et al., 2021). Third, the surface functional groups in the amendments could be involved a complexation reaction with Pb^{2+} (Li et al., 2020). For CT and CSP, the functional groups (e.g., amine and hydroxyl) provided donor ligands and chelation sites for Pb adsorption (Sharma et al., 2022). CSB had abundant C = O groups (Fig. S2D) that likely to form C − O − Pb and/or C = O − Pb complexes during the Pb-biochar interaction (Sun et al., 2021). Overall, CSB had higher pH, ash content, and abundant C = O bonds, leading to the greatest remediation efficiency in Pb immobilization. However, CT rendered little influence on soil pH (Table 1) and did not contain any minerals or metallic elements, thereby resulting in the least effect among all the amendments.

4.3.2. *Arsenic*

The increase of soil As availability after CSP and CSB amendments could be mainly ascribed to the increase in soil pH, DOC, and available P concentration. First, the rising pH increased the negative charge density on soil particles, which in turn liberated the surface-bound/interfacial As ions due to the electrostatic repulsive force between the surface and As species (e.g., $H_2AsO_4^-$, $HAsO_4^{2-}$, and AsO_4^{3-}) (Mensah et al., 2022).

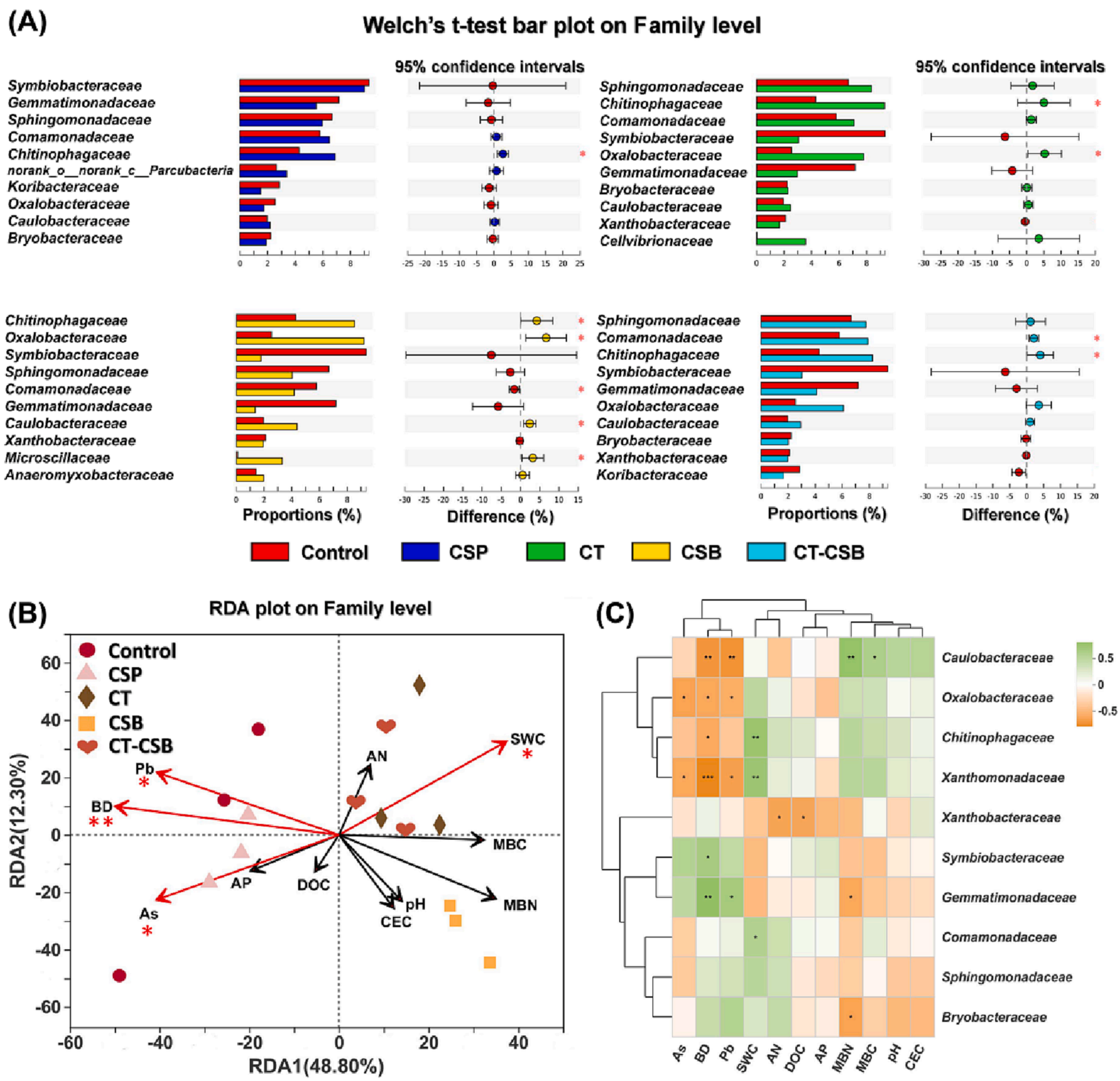

Fig. 6. Variations of the ten most abundant families (A) in different treatment soils; redundancy and analysis (RDA) (B) and Pearson heatmap (C) between environmental factors and Family-level bacterial community. Control: untreated contaminated soil; CSP: crawfish shell powder; CT: chitin; CSB: crawfish shell biochar; CT–CSB: chitin-crawfish shell biochar composite. Arrows represent the environmental variables, and the red arrows indicate significant ($P < 0.05$) factors affecting the bacterial community structure. As: available As; BD: bulk density; Pb: available Pb; SWC: soil water content; AN: available nitrogen; DOC: dissolved organic carbon; AP: available phosphorus; MBN: microbial biomass nitrogen; MBC: microbial biomass carbon; CEC: cation exchange capacity. * represents $P < 0.05$, ** represents $P < 0.01$, and *** represents $P < 0.001$. (For interpretation of the references to colour in this figure legend, the reader is referred to the web version of this article.)

Second, dissolved organic carbon has a strong affinity to As ions to form As–DOC complexes, and the solubilization of DOC resulted in the release of bound As, hence increasing high As availability (El-Naggar et al., 2021). In addition, adsorption competition onto soil particles might occur between negatively charged DOC molecules and As anions (Mensah et al., 2022). The PLS-PM analysis (Fig. 7) revealed that soil chemical properties including pH and DOC had a direct impact on increasing soil As availability and could be a key role in regulating immobilization and translocation of As in the soil–plant system. Third, due to analogous geochemical behavior of P and As, it is also speculated that the increased soil available P content by CSP and CSB amendments might interfere with As binding to soil surface via competition effect (Yang et al., 2023). Although CSP and CSB increased As mobility in soil, the uptake by radish in those treatments decreased. This phenomenon can be explained by two potential aspects: 1) the increased plant biomass after amendments diluted the concentration of absorbed As, i. e., the “dilution effect” (Chen et al., 2020a); 2) As and P shared the same translocator, for instance, the P transporter OsPT1, OsPT4 and OsPT8 of rice was found to be directly involved in As(V) uptake by the root system (Wu et al., 2011; Cao et al., 2017), and high levels of P uptake (Fig. 1C)

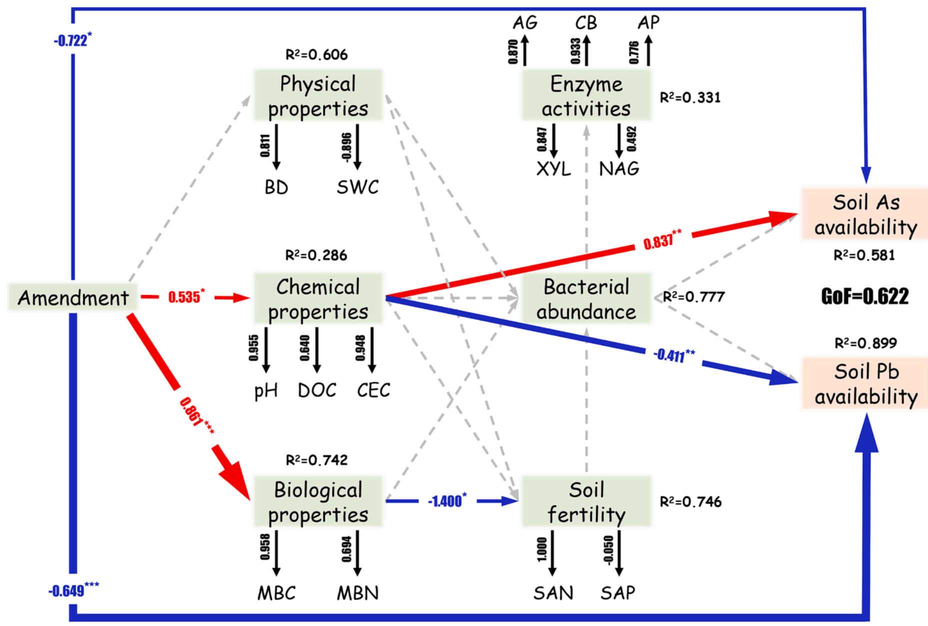

Fig. 7. Partial least squares path model (PLS-PM) showing the effects of amendments on the availability of As and Pb in soils via soil physical/chemical/biological properties, soil fertility, and bacterial abundance. Numbers adjacent to arrows are path coefficients (β), and arrow widths are proportional to the magnitude of the path coefficients. Red and blue arrows indicate positive and negative correlations, respectively. Continuous and dashed arrows indicate significant and insignificant relationships, respectively. Significant level: *: $P < 0.05$; **: $P < 0.01$; ***: $P < 0.001$. BD: bulk density; SWC: soil water content; DOC: dissolved organic carbon; CEC: cation exchange capacity; MBC: microbial biomass carbon; MBN: microbial biomass nitrogen; AG: α-glucosidase; CB: cellobiohydrolase; AP: acid phosphatase; XYL: β-xylosidase; NAG: N-acetyl-β-glucosaminidase; SAN: soil available nitrogen; SAP: soil available phosphorus. (For interpretation of the references to colour in this figure legend, the reader is referred to the web version of this article.)

might reduce As accumulation. On the other hand, the decrease of As bio/phytoavailability in CT-containing treatment might be related to the chitin's surface property. Chitin surface is positively charged owing to protonation of the surface functional groups (e.g., N–H) (Bai et al., 2022) and it likely promoted electrostatic attraction between As and CT to reduce availability of As. In addition, chelation and ion pair formation between protonated amines of CT and As ions likely played an important role in regulating As availability. Chen et al. (2022d) also concluded that electrostatic interaction and complexation are vital mechanisms for the adsorption of As on adsorbents via functional groups.

4.4. Soil enzyme activities

Chitin application enhanced all five enzyme activities (Fig. 5). The enhancement is closely related to the unique nature of CT, serving as an extra source of C and N, offering more suitable habitat conditions (e.g., moisture and aeration) for related microorganisms in soils (Table 1), and promoting their growth and reproduction (as supported by the 16S rRNA gene copy numbers, Table S7).

The CSB-containing treatments significantly reduced AG, XYL and CB activities (Fig. 5). This phenomenon can be attributed to two main aspects: 1) elevated availability of PTEs such as As in soil might deactivate the enzyme proteins (Chen et al., 2020a; Wen et al., 2021); 2) the strong adsorption of biochar to enzyme molecules and/or substrates inhibited the enzyme-substrate reaction (Yang et al., 2022c). In addition, previous studies suggested that certain biochar might contain harmful substances (e.g., heavy metal(loid)s, polycyclic aromatic hydrocarbons (PAHs), and persistent free radicals (PFRs)) (Pan et al., 2023), to cause oxidative damage to microbial activity (Lehmann et al., 2011) and thereby suppressed enzyme activities. To verify this hypothesis, the concentrations of toxic metals, PAHs, and PFRs in CSB were determined. The results indicated that the total concentrations for Cu, Zn, As, Cd, and Pb were 48, 91, 3.2, 0.33, and 2.9 mg kg^{-1}, respectively, with detection of naphthalene (7.5 mg kg^{-1}) and phenanthrene (0.3 mg kg^{-1}) (Table S8). Furthermore, the presence of PFRs (i.e., $\bullet O_2^-$ and $\bullet OH$) was also identified by electron spin resonance (ESR) analysis (Fig. S7). The low application rate (1%) of CSB and the relatively low bioavailability of such toxic substances on biochar may not significantly influence the soil enzyme activities, but their potential effects still cannot be ignored. Moreover, it is assumed that the suppressed activity of acid phosphatase in CSP/CSB-treated soils was mainly associated with the amendment-induced increase of soil pH (Chen et al., 2019), which is in agreement with the negative correlation between soil pH and acid phosphatase activity (r = -0.734, $P < 0.01$).

4.5. Soil bacterial abundance and community composition

Generally, the significant changes in abundance and composition of bacterial community resulting from the immobilization of contaminants were attributed to the adaptation of bacteria to changes in heavy metal contamination levels and environmental conditions. Additions of CT and CT–CSB enhanced the bacterial abundance (Table S7), which could mainly be attributed to amendment-alleviated metal(loid)s stress while providing nutrients and a more favorable environment for bacteria to promote their growth and reproduction. The phylum of Proteobacteria identified as representative gram-negative bacteria is sensitive to carbon sources (Duan et al., 2021). Hence, the enriched Proteobacteria abundance in our study could be associated with the increased DOC in soils (Table 1). Moreover, the added amendments alleviated the toxicity of metal(loid)s to microorganisms, which also facilitated the growth of Proteobacteria. We inferred that the predominating species Proteobacteria might occupy more ecological niches through competitive resource plunder, and thus potentially inhibiting the propagation of other bacterial species such as Acidobacteriota and Chloroflexi phyla.

The enrichment of the family Chitinophagaceae in the CSP, CT, and CT–CSB treatments could be caused by the increased chitin debris from the amendments. Because the members of the Chitinophagaceae are known to degrade polysaccharides such as cellulose and chitin (Hou et al., 2021), and the increased chitin in soils could induce the enhanced activity of Chitinophagaceae. Similar results were found in another study (Hou et al., 2021), in which chitin-rich *Macrobrachium nipponense* was used as a soil amendment. Further, the improved environmental condition could also be responsible for the reproduction of Chitinophagaceae, as validated by the correlation analysis for the CSB treatment (Fig. 6C). Chitin amendment enriched the relative abundance of chitinolytic bacteria, Oxalobacteraceae, suggesting its involvement in the biodegradation of chitin (Hui et al., 2020). Negative correlations between Oxalobacteraceae abundance and soil available As/Pb were recorded (Fig. 6C), suggesting the potential inhibitory effects of metal (loids) on microbial growth. The expansion in the abundances of the families Caulobacteraceae was noted in CSB treatment; this might be attributed to two aspects: 1) the decreased available Pb concentration alleviated the bio-toxicity stress; and 2) the increased MBC and MBN provided extra C/N resources, as suggested by the correlation analysis (Fig. 6C). Moreover, some members of the Caulobacteraceae family (e.g., Brevundimonas nasdae, Au-Bre29 and Au-Bre30) have been identified as As-resistant strains as reported by Yang et al. (2022b), hence it was plausible that the elevated As availability did not inhibit the abundance of Caulobacteraceae in CSB treatment. The family Microscillaceae had a strong extracellular polymeric substance (EPS) secretion capacity to protect cells from toxic pollutants (Chen et al., 2022a). Therefore, its increased abundance in CSB treatment might be a spontaneous stress response to the increased As bioavailability to secrete more EPS for self-protection. Likewise, the enhanced abundance of Comamonadaceae could be related to alleviated As/Pb stress after CT–CSB application and extra C supply, while the decreased Comamonadaceae portion might be attributed to the activated As bioavailability after incorporation of CSB.

4.6. Plant growth

Toxic metal(loid)s can render harmful influences on plant growth by causing oxidative damage to root cells, impeding nutrient uptake and transport, and disrupting plant metabolism (Chen et al., 2022b). Therefore, the decreased As and/or Pb bioavailability to radish was likely the main reason for the increase in plant yield. It is acknowledged that plant growth is positively related to soil fertility. The increased radish biomass could also be due to the improved macronutrient availabilities (i.e., N and P) resulting from direct input and indirect bacteria-driven enhancement of N/P cycles. Meanwhile, amendment applications improved soil properties, i.e., soil moisture, aeration, pH, and CEC (Table 1), which can be beneficial to plant productivity (Dai et al., 2020). Overall, the enhancement of plant yield is the integrated result of internal causes and external conditions, i.e., alleviation of As/Pb stress, improvement of nutrient availability, and amelioration of soil properties.

5. Conclusions

This study concludes that the addition of various amendments (CSP, CT, CSB, and CT–CSB composite) triggered positive impacts on soil physical (bulk density and water content), chemical (pH, CEC, and DOC), biological (MBC and MBN) properties, and nutrient availabilities to varying degrees. CSB was more effective in decreasing Pb availability, which could be attributed to its high pH, ash content, and abundant C = O groups. Through electrostatic interaction and complexation reactions, chitin decreased the soil-available As concentrations by transforming the mobile fractions of As (As_{nsa} and As_{sa}) into stable fractions (As_{cr} and As_{re}). The increased As availability in CSP and CSB treatments was attributed to the amendment-induced elevated soil pH, DOC, and available P content. Therefore, the CT–CSB composite took advantage of both resource materials to minimize the bioavailability of As and Pb and maximize plant yield (65.9% higher than the control). Furthermore, amendment application influenced the bacterial community in terms of abundance and structure, but the effect was dependent on the amendment characteristics and amendment-induced change of soil properties. PLS-PM analysis further highlighted that the amendment applications directly affected soil chemical and biological properties, with the former (i.e., pH, DOC, and CEC) being the strongest predictor for influencing As/Pb availability. In summary, CT–CSB composite can be recommended as an optimal amendment in the treatment of As/Pb co-contaminated arable soil. A physical mixing was adopted in the synthesis of CT–CSB in this study; future research needs to produce chitin-loaded biochar using a cross-linking agent (e.g., glutaraldehyde and sodium alginate) from the perspective of chemical engineering and assess the practical feasibility of such composites in immobilizing toxic metal(loid)s in contaminated soils.

CRediT authorship contribution statement

Hanbo Chen: Conceptualization, Data curation, Investigation, Visualization, Writing – original draft. **Yurong Gao:** Data curation, Investigation, Writing – review & editing. **Huiyun Dong:** Data curation, Software. **Binoy Sarkar:** Writing - review & editing. **Hocheol Song:** Writing – review & editing. **Jianhong Li:** Writing – review & editing. **Nanthi Bolan:** Writing – review & editing. **Bert F. Quin:** Writing – review & editing. **Xing Yang:** Writing – review & editing. **Fangbai Li:** Writing – review & editing. **Fengchang Wu:** Writing – review & editing. **Jun Meng:** Writing – review & editing. **Hailong Wang:** Conceptualization, Supervision, Funding acquisition, Writing – review & editing. **Wenfu Chen:** Writing – review & editing.

Declaration of Competing Interest

The authors declare the following financial interests/personal relationships which may be considered as potential competing interests: Hailong Wang reports financial support was provided by National Natural Science Foundation of China.

Data availability

Data will be made available on request.

Acknowledgments

This study was funded by the National Natural Science Foundation of China (22276031, 21876027), Central Public-interest Scientific Institution Basal Research Fund for Chinese Academy of Tropical Agricultural Sciences (1630022022030), Shenyang Agricultural University Graduate Innovative Cultivation Project (2021YCXB11), the Science and Technology Innovation Project of Foshan, China (1920001000083), and the Key Scientific and Technological Project of Foshan City, China (2120001008392).

Appendix A. Supplementary material

Supplementary data to this article can be found online at https://doi.org/10.1016/j.envint.2023.107989.

References

Ahmad, H.R., Mehmood, K., Sardar, M.F., Maqsood, M.A., Rehman, M.Z.U., Zhu, C., Li, H., 2019. Integrated risk assessment of potentially toxic elements and particle pollution in urban road dust of megacity of Pakistan. Hum. Ecol. Risk Assess. 26, 1810–1831. https://doi.org/10.1080/10807039.2019.1611415.

Ahmed, M.J., Hameed, B.H., Hummadi, E.H., 2020. Review on recent progress in chitosan/chitin-carbonaceous material composites for the adsorption of water pollutants. Carbohydr. Polym. 247, 116690 https://doi.org/10.1016/j.carbpol.2020.116690.

An, T., Chang, Y., Xie, J., Cao, Q., Liu, Y., Chen, C., 2022. Deciphering physicochemical properties and enhanced microbial electron transfer capacity by magnetic biochar. Bioresour. Technol. 363, 127894 https://doi.org/10.1016/j.biortech.2022.127894.

Bai, L., Liu, L., Esquivel, M., Tardy, B.L., Huan, S., Niu, X., Liu, S., Yang, G., Fan, Y., Rojas, O.J., 2022. Nanochitin: chemistry, structure, assembly, and applications. Chem. Rev. 122, 11604–11674. https://doi.org/10.1021/acs.chemrev.2c00125.

Bandara, T., Krohn, C., Jin, J., Chathurika, J.B.A.J., Franks, A., Xu, J., Potter, I.D., Tang, C., 2022. The effects of biochar aging on rhizosphere microbial communities in cadmium-contaminated acid soil. Chemosphere 303, 135153. https://doi.org/10.1016/j.chemosphere.2022.135153.

Cao, Y., Sun, D., Ai, H., Mei, H., Liu, X., Sun, S., Xu, G., Liu, Y., Chen, Y., Ma, L., 2017. Knocking out OsPT4 gene decreases arsenate uptake by rice plants and inorganic arsenic accumulation in rice grains. Environ. Sci. Technol. 51, 12131–12138. https://doi.org/10.1021/acs.est.7b03028.

Carignan, R., Tessier, A., 1988. The co-diagenesis of sulfur and iron in acid lake sediments of southwestern Québec. Geochim Cosmochim Ac 52, 1179–1188. https://doi.org/10.1016/0016-7037(88)90271-2.

Chen, J., Chen, D., Xu, Q., Fuhrmann, J.J., Li, L., Pan, G., Li, Y., Qin, H., Liang, C., Sun, X., 2019. Organic carbon quality, composition of main microbial groups, enzyme activities, and temperature sensitivity of soil respiration of an acid paddy soil treated with biochar. Biol. Fertil. Soils 55, 185–197. https://doi.org/10.1007/s00374-018-1333-2.

Chen, S., Jiang, S., Jiang, H., 2020b. A review on conversion of crayfish-shell derivatives to functional materials and their environmental applications. J. Bioresour. Bioprod. 5, 238–247. https://doi.org/10.1016/j.jobab.2020.10.002.

Chen, D., Wei, Z., Wang, Z., Yang, Y., Chen, L., Wang, X., Zhao, L., 2022a. Long-term exposure to nanoplastics reshapes the microbial interaction network of activated sludge. Environ. Pollut. 314, 120205 https://doi.org/10.1016/j.envpol.2022.120205.

Chen, H., Yang, X., Wang, H., Sarkar, B., Shaheen, S.M., Gielen, G., Bolan, N., Guo, J., Che, L., Sun, H., Rinklebe, J., 2020a. Animal carcass- and wood-derived biochars improved nutrient bioavailability, enzyme activity, and plant growth in metal-phthalic acid ester co-contaminated soils: A trial for reclamation and improvement of degraded soils. J. Environ. Manage. 261, 110246 https://doi.org/10.1016/j.jenvman.2020.110246.

Chen, H., Feng, Y., Yang, X., Yang, B., Biony, S., Bolan, N.S., Meng, J., Wong, J.W.C., Wu, F., Chen, W., Wang, H., 2022b. Assessing simultaneous immobilization of lead and improvement of phosphorus availability through application of phosphorus-rich biochar in a contaminated soil: A pot experiment. Chemosphere 296, 133891. https://doi.org/10.1016/j.chemosphere.2022.133891.

Chen, H., Gao, Y., El-Naggar, A., Niazi, N.K., Sun, C., Shaheen, S.M., Hou, D., Yang, X., Tang, Z., Liu, Z., Hou, H., Chen, W., Rinklebe, J., Pohořelý, M., Wang, H., 2022c. Enhanced sorption of trivalent antimony by chitosan-loaded biochar in aqueous solutions: Characterization, performance and mechanisms. J. Hazard. Mater. 425, 127971. https://doi.org/10.1016/j.jhazmat.2021.127971.

Chen, H., Gao, Y., Li, J., Fang, Z., Bolan, N., Bhatnagar, A., Gao, B., Hou, D., Wang, S., Song, H., Yang, X., Shaheen, S.M., Meng, J., Chen, W., Rinklebe, J., Wang, H., 2022d. Engineered biochar for environmental decontamination in aquatic and soil systems: a review. Carbon Res. 1, 4. https://doi.org/10.1007/s44246-022-00005-5.

Chen, H., Gao, Y., Li, J., Sun, C., Sarkar, B., Bhatnagar, A., Bolan, N., Yang, X., Meng, J., Liu, Z., Liu, Z., Hou, H., Wong, J.W.C., Hou, D., Chen, W., Wang, H., 2022e. Insights into simultaneous adsorption and oxidation of antimonite [Sb(III)] by crawfish shell-derived biochar: Spectroscopic investigation and theoretical calculations. Biochar 4, 37. https://doi.org/10.1007/s42773-022-00161-2.

Cotrufo, M.F., Soong, J.L., Horton, A.J., Campbell, E.E., Haddix, M.L., Wall, D.H., Parton, W.J., 2015. Formation of soil organic matter via biochemical and physical pathways of litter mass loss. Nat. Geosci. 8, 776–779. https://doi.org/10.1038/NGEO2520.

Dai, Y., Zheng, H., Jiang, Z., Xing, B., 2020. Combined effects of biochar properties and soil conditions on plant growth: A meta-analysis. Sci. Total Environ. 713, 136635 https://doi.org/10.1016/j.scitotenv.2020.136635.

Duan, Y., Yang, J., Song, Y., Chen, F., Li, X., Awasthi, M., Li, H., Zhang, L., 2021. Clean technology for biochar and organic waste recycling, and utilization in apple orchard. Chemosphere 274, 129914. https://doi.org/10.1016/j.chemosphere.2021.129914.

Egusa, M., Matsukawa, S., Miura, C., Nakatani, S., Yamada, J., Endo, T., Ifuku, S., Kaminaka, H., 2020. Improving nitrogen uptake efficiency by chitin nanofiber promotes growth in tomato. Int. J. Biol. Macromol. 151, 1322–1331. https://doi.org/10.1016/j.ijbiomac.2019.10.178.

El-Naggar, A., Chang, S.X., Cai, Y., Lee, Y.H., Wang, J., Wang, S.-L., Ryu, C., Rinklebe, J., Sik Ok, Y., 2021. Mechanistic insights into the (im)mobilization of arsenic, cadmium, lead, and zinc in a multi-contaminated soil treated with different biochars. Environ. Int. 156, 106638. https://doi.org/10.1016/j.envint.2021.106638.

Gao, S., Deluca, T.H., Cleveland, C.C., 2019. Biochar additions alter phosphorus and nitrogen availability in agricultural ecosystems: a meta-analysis. Sci. Total Environ. 654, 463–472. https://doi.org/10.1016/j.scitotenv.2018.11.124.

Gao, Y., Fang, Z., Van Zwieten, L., Bolan, N., Dong, D., Quin, B.F., Meng, J., Li, F., Wu, F., Wang, H., Chen, W., 2022. A critical review of biochar-based nitrogen fertilizers and their effects on crop production and the environment. Biochar 4, 36. https://doi.org/10.1007/s42773-022-00160-3.

Gao, Y., Fang, Z., Lin, W., Chen, H., Bhatnagar, A., Li, J., Xie, Y., Bao, Y., Chen, J., Zhao, H., Meng, J., Chen, W., Wang, H., 2023. Large-flake graphene-modified biochar for the removal of bisphenol S from water: rapid oxygen escape mechanism for synthesis and improved adsorption performance. Environ. Pollut. 317, 120847 https://doi.org/10.1016/j.envpol.2022.120847.

Hou, Y., Li, B., Feng, G., Zhang, C., He, J., Li, H., Zhu, J., 2021. Responses of bacterial communities and organic matter degradation in surface sediment to *Macrobrachium nipponense* bioturbation. Sci. Total Environ. 759, 143534 https://doi.org/10.1016/j.scitotenv.2020.143534.

Hou, D., O'Connor, D., Igalavithana, A.D., Alessi, D.S., Luo, J., Tsang, D.C.W., Sparks, D. L., Yamauchi, Y., Rinklebe, J., Ok, Y.S., 2020. Metal contamination and bioremediation of agricultural soils for food safety and sustainability. Nat. Rev. Earth Environ. 1, 366–381. https://doi.org/10.1038/s43017-020-0061-y.

Hui, C., Jiang, H., Liu, B., Wei, R., Zhang, Y., Zhang, Q., Liang, Y., Zhao, Y., 2020. Chitin degradation and the temporary response of bacterial chitinolytic communities to chitin amendment in soil under different fertilization regimes. Sci. Total Environ. 705, 136003. https://doi.org/10.1016/j.scitotenv.2019.136003.

Lehmann, J., Rillig, M.C., Thies, J., Masiello, C.A., Hockaday, W.C., Crowley, D., 2011. Biochar effects on soil biota-a review. Soil Biol. Biochem. 43, 1812–1836. https://doi.org/10.1016/j.soilbio.2011.04.022.

Li, J., Qiu, Y., Zhao, Q., Chen, D., Wu, Z., Peng, A., Niazi, N.K., Trakal, L., Sakrabani, R., Gao, B., Wang, H., Wu, W., 2020. Lead and copper-induced hormetic effect and toxicity mechanisms in lettuce (*Lactuca sativa* L.) grown in a contaminated soil. Sci. Total Environ. 741, 140440 https://doi.org/10.1016/j.scitotenv.2020.140440.

Liu, K., Ran, Q., Li, F., Shaheen, S.M., Wang, H., Rinklebe, J., Liu, C., Fang, L., 2022. Carbon-based strategy enables sustainable remediation of paddy soils in harmony with carbon neutrality. Carbon Research 1, 12. https://doi.org/10.1007/s44246-022-00012-6.

Lu, R., 2000. Analytical Methods for Soil Agrochemistry. Chinese Agricultural Science and Technology Publishing House, (in Chinese), Beijing. ISBN: 9787801199256.

Mehmood, K., Ahmad, H.R., Abbas, R., Saifullah, Murtaza, G., 2019. Heavy metals in urban and peri-urban soils of a heavily-populated and industrialized city: Assessment of ecological risks and human health repercussions. Hum. Ecol. Risk Assess. 26, 1705–1722. https://doi.org/10.1080/10807039.2019.1601004.

Mehmood, K., Bao, Y., Abbas, R., Saifullah, Petropoulos, G.P., Ahmad, H.R., Abrar, M.M., Mustafa, A., Abdalla, A., Lasaridi, K., Fahad, S., 2021. Pollution characteristics and human health risk assessments of toxic metals and particle pollutants via soil and air using geoinformation in urbanized city of Pakistan. Environ. Sci. Pollut. Res. 28 (41), 58206–58220. https://doi.org/10.1007/s11356-021-14436-x.

Mensah, A.K., Marschner, B., Shaheen, S.M., Rinklebe, J., 2022. Biochar, compost, iron oxide, manure, and inorganic fertilizer affect bioavailability of arsenic and improve soil quality of an abandoned arsenic-contaminated gold mine spoil. Ecotoxicol. Environ. Saf. 234, 113358 https://doi.org/10.1016/j.ecoenv.2022.113358.

Pan, Y., Chen, H., Bolan, N., Sarkar, B., Wang, H., Chen, C., 2023. Both sides of the coin: Benefits and crises of biochar in sediment remediation. Rev. Environ. Contam. T. 261, 4. https://doi.org/10.1007/s44169-023-00028-y.

Pan, H., Yang, X., Chen, H., Sarkar, B., Bolan, N., Shaheen, S.M., Wu, F., Che, L., Ma, Y., Rinklebe, J., Wang, H., 2021. Pristine and iron-engineered animal- and plant-derived biochars enhanced bacterial abundance and immobilized arsenic and lead in a contaminated soil. Sci. Total Environ. 763, 144218 https://doi.org/10.1016/j.scitotenv.2020.144218.

Saiya-Cork, K.R., Sinsabaugh, R.L., Zak, D.R., 2002. The effects of long term nitrogen deposition on extracellular enzyme activity in an *Acer saccharum* forest soil. Soil Biol. Biochem. 34, 1309–1315. https://doi.org/10.1016/s0038-0717(02)00074-3.

Shamshina, J.L., Kelly, A., Oldham, T., Rogers, R.D., 2020. Agricultural uses of chitin polymers. Environ. Chem. Lett. 18, 53–60. https://doi.org/10.1007/s10311-019-00934-5.

Sharma, M., Chouksey, S., Gond, L., Bajpai, A., 2022. A hybrid bionanocomposite for Pb (II) ion removal from water: synthesis, characterization and adsorption kinetics studies. Polym. Bull. 79, 10675–10706. https://doi.org/10.1007/s00289-021-04073-2.

Singh, H., Northup, B.K., Rice, C.W., Prasad, P.V.V., 2022. Biochar applications influence soil physical and chemical properties, microbial diversity, and crop productivity: a meta-analysis. Biochar 4, 8. https://doi.org/10.1007/s42773-022-00138-1.

Sirajudheen, P., Poovathumkuzhi, N.C., Vigneshwaran, S., Chelaveettil, B.M., Meenakshi, S., 2021. Applications of chitin and chitosan based biomaterials for the adsorptive removal of textile dyes from water-a comprehensive review. Carbohydr. Polym. 273, 118604 https://doi.org/10.1016/j.carbpol.2021.118604.

Situ, G., Zhao, Y., Zhang, L., Yang, X., Chen, D., Li, S., Wu, Q., Xu, Q., Chen, J., Qin, H., 2022. Linking the chemical nature of soil organic carbon and biological binding agent in aggregates to soil aggregate stability following biochar amendment in a rice paddy. Sci. Total Environ. 847, 157460 https://doi.org/10.1016/j.scitotenv.2022.157460.

Sun, T., Xu, Y., Sun, Y., Wang, L., Liang, X., Jia, H., 2021. Crayfish shell biochar for the mitigation of Pb contaminated water and soil: Characteristics, mechanisms, and applications. Environ. Pollut. 271, 116308 https://doi.org/10.1016/j.envpol.2020.116308.

Tessier, A., Campbell, P.G.C., Bisson, M., 1979. Sequential extraction procedure for the speciation of particulate trace metals. Anal. Chem. 51, 844–851. https://doi.org/10.1021/ac50043a017.

Wang, Y., Zhang, Y., Zhao, H., Hu, W., Zhang, H., Zhou, X., Luo, G., 2022. The effectiveness of reed-biochar in mitigating phosphorus losses and enhancing microbially-driven phosphorus dynamics in paddy soil. J. Environ. Manage. 314, 115087 https://doi.org/10.1016/j.jenvman.2022.115087.

Wen, E., Yang, X., Chen, H., Shaheen, S.M., Sarkar, B., Xu, S., Song, H., Liang, Y., Rinklebe, J., Hou, D., Li, Y., Wu, F., Pohořelý, M., Wong, J.W.C., Wang, H., 2021. Iron-modified biochar and water management regime-induced changes in plant growth, enzyme activities, and phytoavailability of arsenic, cadmium and lead in a paddy soil. J. Hazard. Mater. 407, 124344 https://doi.org/10.1016/j.jhazmat.2020.124344.

Wenzel, W.W., Kirchbaumer, N., Prohaska, T., Stingeder, G., Lombi, E., Adriano, D.C., 2001. Arsenic fractionation in soils using an improved sequential extraction procedure. Anal. Chim. Acta 436 (2), 309–323. https://doi.org/10.1016/s0003-2670(01)00924-2.

Wu, J., Jorgensen, R.G., Pommerening, B., Chaussod, R., Brookes, P.C., 1990. Measurement of soil microbial biomass-C by fumigation-extraction an automated procedure. Soil Biol. Biochem. 22, 1167–1169. https://doi.org/10.1016/0038-0717(90)90046-3.

Wu, Z., Ren, H., McGrath, S.P., Wu, P., Zhao, F., 2011. Investigating the contribution of the phosphate transport pathway to arsenic accumulation in rice. Plant Physiol. 157, 498–508. https://doi.org/10.2307/41435521.

Xie, J., Guo, M., Xie, J., Chang, Y., Mabruk, A., Zhang, T., Chen, C., 2022. COD inhibition alleviation and anammox granular sludge stability improvement by biochar addition. J. Cleaner Prod. 345, 131167 https://doi.org/10.1016/j.jclepro.2022.131167.

Xu, Y., Seshadri, B., Bolan, N., Sarkar, B., Ok, Y.S., Zhang, W., Rumpel, C., Sparks, D., Farrell, M., Hall, T., Dong, Z., 2019. Microbial functional diversity and carbon use feedback in soils as affected by heavy metals. Environ. Int. 125, 478–488. https://doi.org/10.1016/j.envint.2019.01.071.

Yan, N., Chen, X., 2015. Don't waste seafood waste. Nature 524, 155–157. https://doi.org/10.1038/524155a.

Yang, B., Chen, H., Yang, X., Wu, X., Chen, J., Wang, H., 2022a. Effects of different soil amendments on soil nutrient transformation and bioavailability of arsenic and lead in a contaminated soil. J. Soil Water Conserv. 36, 332–345. https://doi.org/10.13870/j.cnki.stbcxb.2022.01.042.

Yang, X., Li, Y., Feng, R., Chen, J., Alwathnani, H.A., Xu, W., Rensing, C., 2022b. Characterization of two highly arsenic-resistant *Caulobacteraceae* strains of *Brevundimonas nasdae*: Discovery of a new arsenic resistance determinant. Int. J. Mol. Sci. 23, 5619. https://doi.org/10.3390/ijms23105619.

Yang, X., Dai, Z., Ge, C., Yu, H., Bolan, N., Tsang, D.C.W., Song, H., Hou, D., Shaheen, S. M., Wang, H., Rinklebe, J., 2023. Multiple-functionalized biochar affects rice yield and quality via regulating arsenic and lead redistribution and bacterial community structure in soils under different hydrological conditions. J. Hazard. Mater. 444, 130308 https://doi.org/10.1016/j.jhazmat.2022.130308.

Yang, R., Su, Y., Aubrecht, K.B., Wang, X., Ma, H., Grubbs, R.B., Hsiao, B.S., Chu, B., 2015. Thiol-functionalized chitin nanofibers for As(III) adsorption. Polymer 60, 9–17. https://doi.org/10.1016/j.polymer.2015.01.025.

Yang, Y., Sun, K., Liu, J., Chen, Y., Han, L., 2022c. Changes in soil properties and CO_2 emissions after biochar addition: Role of pyrolysis temperature and aging. Sci. Total Environ. 839, 156333 https://doi.org/10.1016/j.scitotenv.2022.156333.

Zhang, D., Zhang, K., Chen, K., Xue, Y., Liang, J., Cai, Y., 2022. Mitigation of organic fouling of ultrafiltration membrane by high-temperature crayfish shell biochar: Performance and mechanisms. Sci. Total Environ. 820, 153183 https://doi.org/10.1016/j.scitotenv.2022.153183.

Zhao, Y., Liang, C., Shao, S., Chen, J., Qin, H., Xu, Q., 2021. Linkages of litter and soil C:N: P stoichiometry with soil microbial resource limitation and community structure in a subtropical broadleaf forest invaded by Moso bamboo. Plant Soil 465, 473–490. https://doi.org/10.1007/s11104-021-05028-2.

Zhao, F., Ma, Y., Zhu, Y., Tang, Z., McGrath, S.P., 2015. Soil contamination in China: current status and mitigation strategies. Environ. Sci. Technol. 49, 750–759. https://doi.org/10.1021/es5047099.

Zhu, Y., Wan, L., You, Y., Cheng, Y., Ma, J., Chen, F., 2022. Enhancing network complexity and function of soil bacteria by thiourea-modified biochar under cadmium stress in post-mining area. Chemosphere 302, 134811. https://doi.org/10.1016/j.chemosphere.2022.134811.